



**HAL**  
open science

## NavTEL: an open-source tool for ship routing and underkeel clearance management in estuarine channels

Sylvain Orseau, Nicolas Huybrechts, Pablo Tassi, Sami Kaidi, Fabrice Klein

### ► To cite this version:

Sylvain Orseau, Nicolas Huybrechts, Pablo Tassi, Sami Kaidi, Fabrice Klein. NavTEL: an open-source tool for ship routing and underkeel clearance management in estuarine channels. *Journal of Waterway, Port, Coastal, and Ocean Engineering*, 2021, 147 (2), pp.04020053. 10.1061/(ASCE)WW.1943-5460.0000610 . hal-03257958

**HAL Id: hal-03257958**

**<https://hal.sorbonne-universite.fr/hal-03257958>**

Submitted on 11 Jun 2021

**HAL** is a multi-disciplinary open access archive for the deposit and dissemination of scientific research documents, whether they are published or not. The documents may come from teaching and research institutions in France or abroad, or from public or private research centers.

L'archive ouverte pluridisciplinaire **HAL**, est destinée au dépôt et à la diffusion de documents scientifiques de niveau recherche, publiés ou non, émanant des établissements d'enseignement et de recherche français ou étrangers, des laboratoires publics ou privés.

1                   **NavTEL: an open-source tool for ship routing and underkeel**  
2                   **clearance management in estuarine channels.**

3                   Sylvain Orseau<sup>1</sup>, Nicolas Huybrechts<sup>2</sup>, Pablo Tassi<sup>3</sup>, Sami Kaidi<sup>4</sup>, and Fabrice Klein<sup>5</sup>

4                   <sup>1</sup>Cerema, Direction Technique Eau, Mer et Fleuves, 134 rue de Beauvais - CS  
5                   60039-60280 Margny-lès-Compiègne. Sorbonne Universités, Université de Technologie  
6                   de Compiègne, CNRS, FRE 2012 Roberval, Centre de recherche Royallieu, CS 60 319,  
7                   60203 Compiègne cedex. Email: nicolas.huybrechts@cerema.fr

8                   <sup>2</sup>Cerema, Direction Technique Eau, Mer et Fleuves, 134 rue de Beauvais - CS  
9                   60039-60280 Margny-lès-Compiègne. Sorbonne Universités, Université de Technologie  
10                  de Compiègne, CNRS, FRE 2012 Roberval, Centre de recherche Royallieu, CS 60 319,  
11                  60203 Compiègne cedex.

12                  <sup>3</sup>Electricité de France, R&D Department, 6 quai Watier, BP 49, 78401 Chatou Cedex,  
13                  France. Laboratoire d'Hydraulique Saint Venant (ENPC-EDF/R&D-CEREMA), 6 quai  
14                  Watier, BP 49, 78401 Chatou Cedex, France.

15                  <sup>4</sup>Cerema, Direction Technique Eau, Mer et Fleuves, 134 rue de Beauvais - CS  
16                  60039-60280 Margny-lès-Compiègne. Sorbonne Universités, Université de Technologie  
17                  de Compiègne, CNRS, FRE 2012 Roberval, Centre de recherche Royallieu, CS 60 319,  
18                  60203 Compiègne cedex.

19                  <sup>5</sup>Grand Port Maritime de Bordeaux, 152 quai de Bacalan - CS 41320 – 33082 Bordeaux  
20                  Cedex, France.

## 21 **ABSTRACT**

22 NavTEL is a new decision support tool for the short-term (36 hours) planning of ship  
23 routes and the management of underkeel clearance in estuarine navigation channels.  
24 NavTEL used a deterministic method and is coupled with the TELEMAC-MASCARET  
25 system for numerical modeling of hydrodynamic and sediment transport in the estuary  
26 with a two-dimensional approach. In its present version, NavTEL allows to (i) prepare and  
27 launch daily simulations automatically, and (ii) to post-process simulation outputs to find  
28 the safest ship route and to predict underkeel clearances at specified locations. Because  
29 of the reliability of the results lies on the accuracy of water level predictions, numerical  
30 simulations were performed with measured river discharges, storm surge forecasts and  
31 time-varying friction coefficients for bed roughness. Even though NavTEL was initially  
32 developed for the Atlantic Port of Bordeaux located in the Gironde Estuary, its kernel has  
33 a modular structure allowing to adjust the tool to different port configurations and types  
34 of water bodies. Finally, examples of graphical outputs and reports generated by NavTEL  
35 are shown for an application of a container ship coming into the port of Bordeaux.

## 36 **KEYWORDS**

37 Ship route, Underkeel Clearance Management, Squat, Numerical modelling, NavTEL,  
38 TELEMAC-MASCARET modelling system, Gironde Estuary

## 39 **INTRODUCTION**

40 In the last few decades, maritime transportation has become the most important ship-  
41 ping method with a fourfold growth of the ship traffic over 20 years since early 1900s  
42 (Tournadre 2014). Ship sizes also present an impressive growth and very large container  
43 ships are now commonly used to carry merchandise between ports (Sys et al. 2008). In  
44 this context, a vigorous competition between ports arises to increase their productivity  
45 especially by providing an excellent maritime and hinterland access. This can result in  
46 substantial financial efforts for ports to maintain or deepen the navigation channel. How-  
47 ever, these efforts have lagged behind the growth of ship size.

48 Constraints for the entrance of very large ships in the navigation channel are multi-  
49 ple, particularly for ports located in estuaries where the balance between an efficient and  
50 safe navigation, and the maintenance of the navigation channel is often difficult to en-  
51 sure. In these environments, the navigation of deep-drafted containers is firstly affected  
52 by irregular depth variation and sometimes the presence of shoals. Insufficient water  
53 depth could lead to potential disturbance on the traffic, with significant economic losses,  
54 or worse, a ship grounding. In addition, dynamic ship sinkage or buoyancy also needs to  
55 be predicted carefully. The vertical motions could be modified by (i) the increase of flow  
56 speed under the ship in shallow waters (Vantorre et al. 2017) and the proximity of banks  
57 inducing a drop in pressure (Lataire and Vantorre 2017; Zou and Larsson 2013), and (ii)  
58 the seasonal variation of the salt intrusion length inducing a decrease of the buoyancy  
59 during high river discharge periods (Barrass 2000). For turbid estuaries characterized by  
60 a pronounced Turbidity Maximum Zone (TMZ), fluid mud is commonly observed on the  
61 bottom of the navigation channel. Although navigation through unconsolidated mud lay-  
62 ers are common in several navigation channels, highly concentrated suspension of fine  
63 sediments may lead to a modified ship behavior (Delefortrie et al. 2005; Delefortrie et al.  
64 2010), as well as a ship resistance (Kaidi et al. 2020).

65 Among the large number of parameters that ensure a safe navigation, the UnderKeel  
66 Clearance (UKC) is one of the most important (Parker and Huff 1998). The UKC is defined  
67 as the available space between the ship's keel and the bottom and is often estimated as  
68 10% of the static draft. However, in estuarine navigation channels, the minimal allowed  
69 UKC can be lower due to (i) the navigable depth affected by tide, storm surge and flowrate  
70 variation (ii) the dynamic ship sinkage and (iii) the tidal window referring to the period in  
71 which water levels are sufficient to ensure the safe passing of a ship. These factors can  
72 be accounted by considering, respectively, dredging operations in siltation areas, and  
73 variations of the water density with salinity and suspended particulate matter. Therefore,  
74 UKC maintenance is crucial as it could lead to serious economic consequences if its



determination is inaccurate.

In maritime transport, decision support tool are multiple and used for various applications such as ship routing and scheduling (Kim and Lee 1997; Fagerholt and Lindstad 2007), port selection (Lam and Dai 2012) or ship collision (Lazarowska 2016). To the authors knowledge, few DST have been developed for ship routing and underkeel clearance management in estuarine channels, excepted for some proprietary software such as ProToel. Developed in 2009 by researchers from Ghent University, ProToel is able to determine tidal window and underkeel clearances based on both deterministic and probabilistic approaches (Eloot et al. 2009; Vantorre et al. 2013) for a specific ship. However, the tool does not include a kernel capable to simulate hydro-meteorological conditions, requiring users to provide data from measurements or forecasts at specified locations. The reliability of the route and the accuracy of underkeel clearances depends heavily on forecasts. Therefore, the application of a DST that relies exclusively on the forcing information provided by the user might difficult to plan ship routes, particularly if the period of interest presents missing or incomplete data sets.

Nowadays, logistics in ports and maritime industry has reached a high degree of complexity, requiring for practical reasons the application of analytical methods to objectively support decision-making processes. Ideally, these methods need to be embedded in a collaborative environment in the form of Decision Support Tool (DST), in order to facilitate the required port operations (Mar-Ortiz et al. 2018). The DST currently used by the port of Bordeaux only predicts water levels at a few locations considered most critical via a reconstruction of the tidal signal based on harmonic constituents. The passing hours at these locations were determined empirically and provided by tables depending on the tidal range (low or high), the route (seaward, flood landward or ebb landward) and ship speed. For the arrival of a ship, passing hours were given by tables, while for the departure an optimization procedure was performed to find the best route. The procedure consists to converge to the highest maximum allowable draft and to deduce corresponding passing

102 times.

103 The purpose of this study is to develop an efficient DST combining the hydrodynam-  
104 ics and sediment transport modules of the open-source TELEMAC-MASCARET mod-  
105 elling system ([www.opentelemac.org](http://www.opentelemac.org)) and Python scripts, encapsulated in a framework  
106 capable to efficiently manage the UKC and to assist port authorities in the planning  
107 and the safe conduct of ship transit. Enhanced features of the DST are (i) its abil-  
108 ity to provide depth-averaged velocity and water density in addition to the water level,  
109 and (ii) the using of measured river discharges and near-real time forecasting of storm  
110 surge at boundary conditions. The tool is available as an open-source code at <https://gitlab.com/orseausy/navtel> and is presently in an evaluation phase for the Port of  
111 Bordeaux in France.  
112

## 113 **THE PORT OF BORDEAUX AND THE GIRONDE ESTUARY**

114 The tool was developed as part of the Gironde XL 3D project which aims at increasing  
115 the actual knowledge of the sediment dynamics inside the Gironde Estuary and to develop  
116 a set of numerical tools to assist the Port Authority in a better regulation and coordination  
117 of ship transits. The Atlantic Port of Bordeaux is located in the Gironde estuary and is  
118 France's 7th largest seaport. It gathers 7 specialized terminals along the estuary with the  
119 most upstream terminal located 100 km inland (Fig. 1b). The foreign maritime traffic reach  
120 an annual average of  $8.5 \times 10^6$  tons and is mainly represented by tankers with 52% of the  
121 overall traffic. A navigation channel of 130 km length and from 150 m to 300 m width con-  
122 nects each terminal and is maintained at a depth of 7 m mean lower low water (MLLW). For  
123 a period comprised between 2015 and 2016, the annual average of dredged volumes was  
124 approximately  $9.5 \times 10^6$  m<sup>3</sup> and was mainly realized by a trailing suction hopper dredger.

125 The Gironde Estuary is a macrotidal and convergent estuary, about 75 km long and  
126 12 km wide at the estuary mouth, dominated by the tide and mainly fed by two tributaries:  
127 the Dordogne River and the Garonne River (Fig. 1b). These tributaries are characterized  
128 by a total catchment area of approximately 83 000 km<sup>2</sup>. During the 2005-2014 period,

129 mean total discharges were  $1100 \text{ m}^3 \text{ s}^{-1}$  in winter and  $295 \text{ m}^3 \text{ s}^{-1}$  in summer (Jalón-Rojas  
130 et al. 2015). The tide is a semi-diurnal type and the mean neap and spring tidal ranges  
131 are of 2.5 and 5 m, respectively (Bonneton et al. 2015). Water levels are measured at 9  
132 tidal gauges placed along the estuary from Le Verdon to Bordeaux stations.

133 The hydrodynamics of the Gironde Estuary is mainly forced by tide and freshwater  
134 runoff while the influence of winds is not clearly determined. Along the estuary, tidal  
135 and subtidal water level variations depict an amplification mainly explained by tidal pro-  
136 cesses (Ross and Sottolichio 2016). The tide is also characterized by a flood-dominated  
137 asymmetry. However, the continuous decrease of the river discharge observed over the  
138 past 60 years induced strong changes in tidal range and tidal distortion (Schmidt 2016;  
139 Jalón-Rojas et al. 2018).

140 From the port of Bordeaux to the estuary mouth, the bed composition can be dis-  
141 tributed over 3 areas: (i) a mixed facies dominated by mud (56% of clays, 42% of silts and  
142 2% of sands) between Bordeaux and the confluence of the Dordogne and the Garonne  
143 rivers, (ii) a mixed facies in the central estuary up to Richard and (iii) a sandy facies in the  
144 lower estuary and the estuary mouth. Fine suspended-sediments formed a turbidity max-  
145 imum zone (TMZ) due to the combined action of the tidal asymmetry and vertical density  
146 gradients (van Maanen and Sottolichio 2018). Inside this zone, suspended-particulate  
147 matter (SPM) concentrations can vary between 1 and  $10 \text{ g L}^{-1}$  (Sottolichio and Castaing  
148 1999). The TMZ location changes seasonally with hydrological conditions and is formed  
149 in the upper estuary during summer-autumn (Doxaran et al. 2009). With increasing fresh-  
150 water inflows, TMZ shifts to the central estuary and a part can be exported to the ocean  
151 during peak floods. River flow discharges from the Garonne and Dordogne rivers have  
152 also a strong effect on the persistence and the concentration of the TMZ (Jalón-Rojas  
153 et al. 2015). Sottolichio and Castaing (1999) also noticed the presence of a secondary  
154 TMZ in the middle estuary (near Pauillac in the Fig. 1b) induced by strong local resuspen-  
155 sions.

## 156 THE NAVTEL FRAMEWORK

157 The NavTEL decision support tool determines near real-time ship route and underkeel  
158 clearance by predicting water levels, current velocities and water density along an estuar-  
159 ine navigation channel. Because of its modular structure, the tool can be easily adjusted  
160 to a different port configuration. The kernel of NavTEL is composed by 2 modules named  
161 NAVIRE and TELBOT (Fig. 2). The TELBOT module prepares and launches simulations,  
162 while the NAVIRE module post-processes simulation results to determine the route and  
163 predict the squat. Additionally, NAVIRE incorporates time-varying friction coefficients for  
164 bed roughness. To ensure portability, NavTEL can be steered from the command line and  
165 does not include a graphical user interface. A description of each module of NavTEL is  
166 presented thereafter.

### 167 **TELBOT module: to predict hydrological and water-density conditions**

#### 168 *The TELEMAC-MASCARET modelling system*

169 To predict the hydrodynamics and the sediment transport, the TELBOT module lies  
170 on two modules of the TELEMAC-MASCARET modeling system (TMS). TELBOT uses  
171 the hydrodynamics (TELEMAC-2D) and sediment transport (SISYPHE) modules. The  
172 former is dedicated to the simulation of free-surface flows and computes at each nodes  
173 water levels and flow velocity components. It also accounts bed friction, meteorological  
174 forcings such as atmospheric pressure and wind, and longitudinal salinity gradients. The  
175 latter is dedicated to the sediment transport (bed-load, suspended-load or total load) and  
176 bed evolution. It also accounts processes specific to cohesive sediments like the self-  
177 weight consolidation. The assessment of the TMS has been demonstrated through its  
178 application on a large number of coastal and estuarine cases (Bi and Toorman 2015;  
179 Brown and Davies 2010; Santoro et al. 2013; Van 2012). In this work, only suspended  
180 sediment transport processes are considered.

181 The hydrodynamics module is based on the solution of the 2D nonlinear depth-averaged  
182 shallow water equations by using the finite element or the finite volume approaches (Her-

183 vouet 2007). The sediment transport module solves the depth-averaged sediment con-  
184 centration equation. Due to the short time scale considered for the numerical simulations,  
185 bed evolution is not accounted in the current version of NavTEL.

186 The 2D hydrodynamic model was calibrated automatically by finding time-varying bed  
187 friction coefficients depending river discharges. Water levels are predicted with accuracy,  
188 particularly during low river discharge periods with a maximum Root Mean Square Error  
189 (RMSE) below 20 cm at Bordeaux. However, during high river discharge periods, the  
190 robustness of the model might decrease due to the influence of the TMZ on the estuarine  
191 bed structure (Jalón-Rojas et al. 2018). In order to provide accurate predictions for highly  
192 variable hydrological conditions, special attention is paid to the influence of the seasonal  
193 variation of the river discharge for determining the bed friction coefficients used in the  
194 hydrodynamics module.

### 195 *Numerical Model Setup*

196 The numerical domain extends over an area of 2200 km<sup>2</sup> from the maritime part to the  
197 limit of the tide influence 170 km upstream in the Dordogne and Garonne rivers. The mesh  
198 is unstructured, composed of triangular elements and is refined at the navigation channel,  
199 fluvial areas and at the estuary mouth. Element sizes range from 300 m in the maritime  
200 part to 80 m in refined areas to better characterize the flow patterns.

201 Numerical simulations are performed for a period of 18 days including a spin-up period  
202 of 15 days and a forecast period of 3 days from the date of the request. The spin-up period  
203 allows to distribute salinity and suspended-sediments depending hydrological conditions  
204 to reach a state with the correct salt intrusion length and the right location of the TMZ.  
205 However, the salinity field has to be initialized at time  $t = 0$  depending freshwater inflow.  
206 For this, the estuary was divided into 4 zones of constant salinity. For each zone, an  
207 empirical relationship with river discharge was established and allows to automatically set  
208 salinity values. To reproduce the formation of TMZ,  $2.6 \times 10^6$  tons of mud were placed in  
209 the central estuary (Fig.1e) as proposed by Sottolichio and Castaing (1999).

210 For the maritime boundary, astronomical tides are reconstructed from tidal atlases in-  
211 cluding 46 harmonic constituents (Pairaud et al. 2008) and are coupled with a large-scale  
212 storm surges model from Météo-France combining the barotropic version of HYCOM code  
213 and the atmospheric model ARPEGE. The storm surge values are provided every hour  
214 near the Cordouan station (Lat: 45.5915, Lon: -1.4303, Fig. 1c). For fluvial boundaries,  
215 measured river discharges were imposed during the spin-up period, while the average of  
216 the last 5 days were used for the forecast period.

217 The bottom friction is parameterized by the Manning-Strickler formulation, distributed  
218 over 7 zones depicted in Figure 1c. During the simulation, friction coefficient values  $K$  are  
219 modified automatically by empirical laws depending the variation of river discharge. Their  
220 values may also be set constant by the user.

### 221 *TELBOT Workflow*

222 The TELBOT module is composed by a set of Python subroutines and bash scripts  
223 used to prepare and launch simulations.

224 The first step consists in creating the TELEMAC-2D and SISYPHE steering files con-  
225 taining numerical and physical information such as the time-step, the friction coefficient  
226 and the eddy viscosity parameterization, as well as the input/output filenames. These file-  
227 names referred to the mesh (binary file), the boundary conditions (ASCII file), result files  
228 (binary file) and optional data files (ASCII format). The second step is to create optional  
229 data files containing river discharge and storm surge values. River discharges are down-  
230 loaded on the national website <https://www.vigicrues.gouv.fr/> in xml format at the Pessac  
231 and La Réole stations located at fluvial boundaries. The same procedure is applied to  
232 obtain storm surge values near the Cordouan station (Fig. 1b).

233 Once all required files are created, simulations are performed and numerical results  
234 are stored in a binary filename SELAFIN (slf format). Model results are kept up to 3 days  
235 before deletion and are available to be used by the NAVIRE module to determine the ship  
236 route and underkeel clearances.

## NAVIRE: to plan routes and to manage underkeel clearance (UKC)

### *Route Planning*

Planning the traffic in the navigation channel is of major interest for port authorities to ease decision making process and therefore improve their productiveness. It might consist on providing precise information about tidal windows and delivering a panel of routes including the safest choice. Following guidance, the ship's master will be able to choose the most convenient ship's passage and anticipate the minimum UKC recommended by the port.

In NAVIRE, route planning lies on the prediction of water levels obtained from the astronomical tide and storm surge forecasts computed by the module TELBOT. This prediction allows to determine the minimal water depth requirement at selected locations (Fig. 1b) for safe passage and thus to delimit the tidal window. Depending on the longitudinal variation of the ship speed, different routes and corresponding passing hours can be provided by the port authorities. In order to find the safest route for ship coming into or leaving the port, an optimization procedure based on the convergence to the highest maximum allowable draft is then performed. For undocumented estuarine channels, the longitudinal variations of the ship speed can be established based on the Automatic Identification System (AIS) tracking system and for different hydrological conditions.

### *Prediction of squat and management of underkeel clearance*

The specification of the maximum allowable draft and minimum UKC required by the port is a subtle balance between financial benefits by optimizing ship traffic and the insurance of a safe navigation to avoid delays or grounding. UKC varies along the ship route and is determined by the charted depth, water level and the dynamic draft considering the ship squat. The ship squat is defined as the sinkage of the ship due to pressure variations along the hull and exacerbated in shallow waters (Debaillon 2010). UKC can be formulated on either deterministic or probabilistic approaches. For a deterministic approach, the value of the water depth minus the static draft of the ship or *gross UKC* is determined

264 by the channel dimensions and the ship speed range. For a probabilistic approach, the  
265 gross UKC is based on an acceptable probability of bottom touch. For NAVIRE, the de-  
266 terministic approach was adopted.

267 To ensure a minimum water depth, the UKC can be estimated using only the static draft  
268 and predicted water level. However, changes in the channel configuration and the water  
269 density, particularly marked in estuarine channels, can produce upward or downward  
270 vertical forces inducing different values of squat. Provide a squat prediction even with  
271 a simple formulation seems crucial to inform the pilots on the risks. Predictions of ship  
272 squat are mainly govern by channel and ship dimensions, and the relative speed of the  
273 ship in water (Barrass and Derrett 2012). Along an estuarine channel, cross-sections  
274 are generally variable and can be characterized as (i) unrestricted channels, (ii) restricted  
275 channels or (iii) canals (Briggs et al. 2009). These channel types differ according to their  
276 proximity to the channel margins and bottom position, width, and bank slopes. In most  
277 cases, the ship squat is expected to vary as the square of the relative speed of the ship  
278 in water (Briggs et al. 2009) and becomes significant when the ratio between the water  
279 depth to the ship draft is  $< 1.5 - 2$ .

280 In NAVIRE, the squat is determined by empirical formulas recommended by the Per-  
281 manent International Association of Navigation Congresses (PIANC) during the design-  
282 ing of a navigation channel (Briggs et al. 2009). These formulas can be divided into two  
283 groups, according to the phases of the design process, namely the concept design phase  
284 and the detailed design phase. The first group includes simple formulations from the In-  
285 ternational Commission for the Reception of Large Ships (ICORELS), Barrass (Barrass  
286 1979) and Yoshimura (Yoshimura 1986). The second group includes formulations to eval-  
287 uate the squat and to perform a statistical analysis such as Eryuzlu (Eryuzlu et al. 1994),  
288 Huuska/Guliev (Huuska 1976) or Römisch (Römisch 1989). These formulations provide  
289 predictions of squat at the bow  $S_B$ , excepted the Römisch formulation which gives squat at  
290 the stern  $S_S$ . However, the use of these formulas are constrained by the channel type and



291 dimensionless parameters describing ship dimensions relative to the channel dimensions.  
292 The user should be informed of these constraints and the relevance of their applications  
293 when predicting the squat. In some cases, these constraints can be severely restrictive.

The computed squat values can be adjusted by accounting the effect of the water density. For this, we consider that the vertical density gradient follows a profile comprised between a linear and a quadratic approximation (Ali et al. 2018; Kaidi et al. 2020). The following equations were obtained for a container ship model (KCM) and are used by NavTEL to predict the minimum and maximum sinkage ( $S_1$  and  $S_2$ , respectively) with the density effect. However, in its current version, NavTEL cannot adjust the squat for other ship categories.

$$S_1 = S_0 + \alpha_1 \Delta\rho \quad (1a)$$

$$S_2 = S_0 + \alpha_2 \Delta\rho \quad (1b)$$

294 where  $S_0$  is the reference sinkage computed with only the dimensions of the ship and  
295 the channel,  $\Delta\rho$  is the density gradient, and  $\alpha_1$  and  $\alpha_2$  are coefficients depending on the  
296 ship's hull form. For the container ship model (KCM), the values of these coefficients are  
297 of  $1.35 \times 10^{-3} \pm 3.8\%$  and  $9 \times 10^{-4}$ , respectively.

### 298 *NAVIRE Workflow*

299 The NAVIRE module is composed of Python scripts used to post-process numerical  
300 model results, to find the optimal route and to determine the underkeel clearance with the  
301 static or the dynamic draft.

302 The communication between the port authority and ships is based on email exchanges  
303 (Fig. 2). The first step consists to query received emails at the address specified by the  
304 user. In this way, the user can choose different requests (emails) for the specified simula-  
305 tion. Emails must contain criteria for navigation (date, hour, destinations and routes) and  
306 for the ship (type, length, width, static draft and speed). Once the required specifications

307 are automatically extracted from the body of the email, NavTEL postprocesses the numer-  
308 ical model results. The tool extracts the hydro-sedimentary variables, e.g. water depth,  
309 water surface elevation, flow velocity, salinity, and mass-concentration at a given interval  
310 (set by default equal to 5 minutes for the current version of NavTEL) of the simulation over  
311 the computational domain.

312 Depending on the shipping route, e.g. landward or seaward, NAVIRE will determine  
313 the passing time at each location and extract the hydro-sedimentary variables. With the  
314 chart datum and the static draft information, a first estimation of the underkeel clearance  
315 at each stations is provided. Optional variables can be used in the model to improve  
316 the determination of underkeel clearances, for example by considering the water density  
317 to predict the squat. Once the computation of the underkeel clearance is performed,  
318 NAVIRE generates a route report in pdf format including passing time, water level, water  
319 density, and underkeel clearance at selected locations.

## 320 **MODEL PERFORMANCE**

321 The ability of the numerical model at reproducing water levels is assessed based on  
322 the Mean Square Error (MSE). To this goal, the configuration considering only astronom-  
323 ical tides (AT) and the NavTEL configuration considering astronomical tides, predicted  
324 storm surges, measured river discharges and time-varying friction coefficients for bed  
325 roughness (NavTEL) were considered:

$$326 \quad \text{MSE}(f, x) = \frac{1}{N} \sum_n^N (f_n - x_n)^2 \quad (2)$$

327 where  $f_n$  is the prediction,  $x_n$  is the measured water levels, the Root Mean Square Error  
328 (RMSE):

$$329 \quad \text{RMSE}(f, x) = \sqrt{\text{MSE}(f, x)} \quad (3)$$

330 and the Skill Score (SS):

$$331 \quad \text{SS} = \left( 1 - \frac{\text{MSE}(f, x)}{\text{MSE}(r, x)} \right) \quad (4)$$

332 where  $r$  is the average of measured water levels over the observation period (Murphy and  
333 Epstein, 1989).

334 The period used to assess the model performance was determined based on the avail-  
335 ability of storm surges information and covered a six months period of 2015 (from 04/01  
336 to 11/01). This period does not includes river floods usually observed between December  
337 and May, but river discharges ranged from 125 to 2860  $\text{m}^3 \text{s}^{-1}$  providing varied hydrological  
338 conditions to demonstrate the robustness of the model. For the overall period, the storm  
339 surge has averaged  $-5.2 \text{ cm}$  and described storm events on 05/05, 08/24 and 09/16 with  
340 values above 30 cm.

341 Comparison between measured and predicted water levels were performed using tidal  
342 gauge records at 9 stations distributed along the navigation channel (Fig. 1b). For clarity,  
343 only Le Verdon, Pauillac and Bordeaux stations are showed in Figures 3 and 4. These  
344 stations were chosen for their locations covering the whole navigation channel and thus  
345 the propagation of tide up to the most upstream terminal (Bordeaux station).

346 At the Verdon station, near the estuary mouth, both the AT and NavTEL configurations  
347 provide accurate predictions of water level for the overall period, with RMSEs of 13 and  
348 15 cm and SS values of 0.99 and 0.98, respectively (Fig. 3a, d). For the AT configura-  
349 tion, the water level predictions are accurate, but tidal ranges are slightly overestimated  
350 inducing maximum errors at high and low tides. A similar observation can be made for  
351 the NavTEL configuration, particularly for high river discharges where differences with  
352 the AT configuration are highest. However, the integration of predicted storm surges in  
353 the NavTEL configuration allows to reproduce the abnormal variation of seawater. For a  
354 deepwater terminal such as the Verdon station, this improvement is not crucial, but for  
355 further downstream and depth-limited terminals like Pauillac station, surge storms can  
356 have an enormous impact on the accurate prediction of the water depth due to channel  
357 convergence and shallow-water effects.

358 At the Pauillac station, errors increase for both the AT and NavTEL configurations, with

359 RMSE values of 19 and 20 cm and skill score (SS) values of 0.98, respectively. For the AT  
360 configuration, high waters levels are better predicted than low waters levels. At Le Verdon  
361 station, the NavTEL configuration tends to overestimate high and low water levels, where  
362 maximum level differences with measurements are observed during flood periods, with  
363 values up to 87 cm.

364 At the Bordeaux station, located approximately 150 km downstream the Cordouan sta-  
365 tion, the integration of multiple harmonic constituents in both numerical simulations al-  
366 lowed to accurately reproduce the tidal asymmetry. For the AT configuration, water levels  
367 are overestimated for high water levels, and underestimated for low water levels (Fig. 3c),  
368 with a RMSE a value of 31 cm and a SS of 0.96. For the NavTEL configuration, the RMSE  
369 value is equal to 22 cm, a value close to that computed for the Pauillac station (Fig. 3f),  
370 and a SS of 0.98. Possible factors that influence a better water level prediction are (i)  
371 the integration of measured values for river discharges that affect tidal damping into the  
372 model, (ii) the accounting of the storm surge information, and (iii) the time-varying friction  
373 coefficients depending on river discharges which allows a better representation of the tide  
374 propagation and therefore a more accurate estimation of the tidal range.

375 Computed RMSEs at selected stations are presented in Table 1. For the AT configura-  
376 tion, errors increase continuously, inducing a maximum RMSE of 31 cm and a minimum SS  
377 of 0.96 at the Bordeaux station. For all stations, more accurate predictions are obtained  
378 in the estuary mouth zone, e.g. at Le Verdon station. For the NavTEL configuration, SS  
379 values never decrease below 0.98 and RMSE values are more homogeneous along the  
380 navigation channel, with values ranging between 15 and 22 cm. This observation suggests  
381 little variation of the accuracy of water level predictions respected to the hydrological con-  
382 ditions.

383 Predictions with the NavTEL configuration are at least as accurate as the configuration  
384 currently used by the GPMB for the lower and the intermediate estuary, but better repro-  
385 duce water level variations in the upper estuary depending meteorological and hydrolog-

386 ical conditions. Similar behaviour is found for the tidal phase, as shown in Fig. 4. The  
387 Verdon and Pauillac gauging stations do not show significant improvements with, respec-  
388 tively, 58% and 46% of high waters that are better predicted by the NavTEL configuration.  
389 However, for high waters have occurred during a period with a total river discharge supe-  
390 rior to  $900 \text{ m}^3 \text{ s}^{-1}$  (averaged over the last six decades), previous rates increase to 60%,  
391 64% and 85% for Le Verdon, Pauillac and Bordeaux stations, respectively. This result  
392 highlights the influence of measured river discharges and time-varying friction coefficients  
393 in the numerical simulations, allowing a better parameterization of the flow resistance and  
394 therefore a more accurate representation of the tidal wave celerity. It also confirms that  
395 NavTEL is more suited for a large range of hydrological conditions, while the actual con-  
396 figuration used by the GPMB provides equivalent or slightly better predictions only for low  
397 river discharges.

## 398 **APPLICATION FOR A SHIP COMING INTO THE PORT OF BORDEAUX**

399 In coastal and river channels, ship navigation is generally allowed for a minimum UKC  
400 of 10% of the static draft. However, in estuaries the presence of soft bottom allows to  
401 reduce this value to 0.8 m. Based on these restrictions, a tidal window is determined and  
402 stored in html format for easy and clear reading (Fig. S1). This information aims to assist  
403 pilots in their decisions for the planning of the optimal ship route. It contains passing hours  
404 of all possible routes at 5-min intervals and corresponding underkeel clearances. NavTEL  
405 also generates a report in pdf format (Fig. S2) containing the suggested passing hours at  
406 selected locations to ensure a safe transit along the channel. It also provides predictions  
407 of water level, underkeel clearance and water density considering salinity and suspended  
408 particulate matter.

409 As an example, NavTEL is applied for an operation requesting the arrival of a container  
410 ship at the Bassens terminal (Fig. 1b) on date 03/20/2020 at 17:30. It has a length of  
411 134 m, a breadth of 23 m, a static draft of 8.3 m, and a block coefficient of 0.6. The variation  
412 of ship speed is included in the passing hours determined empirically by the port and is

413 assumed to be  $\leq 12$  knots.

414 The temporal mean of the salinity over the numerical domain is provided to evaluate  
415 the salt intrusion length and possible density effects on sinkage during the forecast period.  
416 From the 03/19 to the 03/21, the mean limit of the salt intrusion is located in the lowest  
417 estuary downstream the Richard station (Fig. 5). The proposed location seems to be  
418 consistent with hydrological conditions characterized by the averaged value of the total  
419 river discharge of the forecast period (equal to  $1354 \text{ m}^3 \text{ s}^{-1}$  for this example).

420 According to the tidal window, the earliest and the latest time to enter into the estuary  
421 are 12:37 and 15:47 respectively, for date 03/20 (Fig. S1). Based on UKCs, the optimal  
422 route started at 14:17 with a maximum allowable draft of 9.88 m at Pachan station (Fig. 1b).  
423 These observations are confirmed by the graphical output displaying the variation of the  
424 allowable draft along the navigation channel and for the predicted period (Fig. 6). Figure 6  
425 assists pilots in their decisions by quickly visualizing the tidal windows, showing the static  
426 draft on red lines as well as the entire route and the departure time of the safest path  
427 on the black line. The location where the maximum allowable draft was found is also  
428 displayed along the line. Furthermore, it shows that Pauillac and Pachan are the selected  
429 locations which determines if a ship can safely navigate within the Gironde Estuary, as  
430 the length of tidal windows are generally short for the given navigability condition. It is  
431 therefore important to accurately predict the water levels at different stations located on  
432 the ship route, in order to optimize the length of the tidal window.

433 The route report (Fig. S2) provided by NavTEL indicates a transit time of 3 hours and  
434 53 minutes and a hour of arrival 40 minutes after the high tide at the Bordeaux station.  
435 During the transit, highest water levels are observed at downstream stations e.g. from  
436 B12A to By stations, ensuring a navigation at high water and at the beginning of the ebb  
437 phase. During this navigation phase the flow velocity is decreased until the high water  
438 slack occurrence, easing the berthing operation. The lowest underkeel clearances are  
439 identified at Pachan and Pauillac stations (Fig. 1) with values of 1.6 m and 1.7 m, respec-

440 tively. As shown in Fig. 7d, squat values predicted with the Yoshimura formulation are  
441 approximately equal to 0.8 m for all stations.

## 442 **CONCLUSIONS AND PERSPECTIVES**

443 In this study, NavTEL, a new decision support tool to assist pilots and port authori-  
444 ties in the planning of ship route and the management of the underkeel clearance was  
445 introduced. Its originality lies in a combination of numerical tools and Python scripts dedi-  
446 cated to the automation of simulations and the post-processing of outputs to obtain water  
447 level, current velocity, salinity and water density for a given water body. In its current ver-  
448 sion, NavTEL is based on a deterministic approach to compute the hydrodynamics and  
449 sediment transport in an estuarine zone for short-term navigation plannings. To obtain  
450 accurate predictions of the water level, the tool retrieves measured river discharges and  
451 storm surge forecasts. Results highlight the versatility of NavTEL to predict the range  
452 and phase of a tide for various hydrological conditions along the navigation channel. An  
453 application for the port of Bordeaux shows different NavTEL's outputs, in particular the  
454 determination of the tidal window with possible navigable routes, as well as a navigation  
455 report providing passing hours at selected locations for the safest route and correspond-  
456 ing underkeel clearances.

457 Even though NavTEL was initially developed for the Atlantic Port of Bordeaux, its ker-  
458 nel has a modular structure allowing to adjust the tool to different port configurations and  
459 types of water bodies. Further developments include long-term planning of ship route  
460 based on a probabilistic approach, ship manoeuvrability and statistical analysis of the  
461 simulation output to estimate uncertainty predictions.

462 **Acknowledgments**

463 The development of NavTEL was enabled by funding from the Connecting Europe  
464 Facility (CEF) – Transport Sector under agreement (Innovation and Networks Executive  
465 Agency) No. INEA/CEF/TRAN/M2014/1049680 through the project Gironde XL. The au-  
466 thors thanks Météo-France and the Service Hydrographique et Océanographique de la  
467 Marine (SHOM) for providing storm surge and weather forecasts.



468  
469  
470  
471  
472

## **SUPPLEMENTAL DATA**

As an example, NavTEL provides following possible routes with corresponding maximum allowable draft (Fig. S1) and a route report containing relevant informations for navigation (Fig. S2). Both files are available online in the ASCE Library ([ascelibrary.org](http://ascelibrary.org)).

# ROUTE REPORT

473

Date	20/03/20	Static draft:	8.3
Destination:	BASSENS AVAL	High tide at referent harbor:	17h30
Route:	FLOOD LANDWARD	Maximum allowable draft:	9.88
Speed:	12	Tidal coefficient:	50

KP	Critical Locations	Date	Hour	Z	Water Level	UKC	Density	Squat
92.75	B12A	20/03	14h17					
77.8	B20	20/03	14h51					
75.9	RICHARD	20/03	14h57	7.4	4.64	3.0	998.3	0.8
71.5	B25	20/03	15h09					
70.7	GOULEE	20/03	15h12	7.2	4.65	2.8	998.3	0.8
70.4	BY	20/03	15h13	7.0	4.51	2.4	998.3	0.8
68.5	B29	20/03	15h18					
64.8	LAMENA	20/03	15h29	7.1	4.44	2.5	998.3	0.8
63.0	Lamena	20/03	15h34					
59.8	LA MARECHALE	20/03	15h43	7.1	4.41	2.4	998.3	0.8
56.9	SAINT ESTEPHE	20/03	15h52	7.3	4.36	2.6	998.3	0.8
47.3	PAUILLAC	20/03	16h19	6.3	4.49	1.7	998.3	0.8
47.0	Port Plaisance Pauillac	20/03	16h19					
43.8	SAINT JULIEN	20/03	16h28	6.4	4.48	1.8	998.3	0.8
41.5	BEYCHEVELLE	20/03	16h35	6.7	4.49	2.1	998.3	0.8
38.3	CUSSAC	20/03	16h44	6.9	4.49	2.3	998.3	0.8
35.8	Ile Verte	20/03	16h50					
35.7	ILE VERTE	20/03	16h51	7.4	4.39	2.7	998.3	0.8
30.9	ROQUE DE THAU	20/03	17h02	7.8	4.36	3.1	998.3	0.7
26.9	BEC AVAL	20/03	17h13	6.7	4.3	1.9	998.3	0.8
25.7	Potence Bec	20/03	17h15					
24.1	BEC AMONT	20/03	17h19	6.8	4.29	2.0	998.3	0.8
20.4	Esso	20/03	17h27					
19.4	BELLERIVE	20/03	17h32	6.7	4.28	1.9	998.3	0.8
18.8	PACHAN	20/03	17h35	6.4	4.28	1.6	998.3	0.8
17.4	CAILLOU	20/03	17h42	6.6	4.29	1.8	998.3	0.8
16.8	B66	20/03	17h44					
12.3	GRATTEQUINA	20/03	18h02	7.4	4.28	2.6	998.3	0.8
10.0	BASSENS AVAL	20/03	18h10	7.4	4.29	2.6	998.3	0.8
10.0	B67	20/03	18h10					

## REFERENCES

- Ali, M., Kaidi, S., and Lefrancois, E. (2018). "Effect of the muddy area on the surface wave attenuation and the ship's squat." *Proc. 39th Ibero-Latin American Congress on Computational Methods in Engineering.*, Compiègne, France.
- Barrass, B. (2000). *Ship Stability: Notes and Examples*. Elsevier Science.
- Barrass, C. (1979). "The phenomenon of ship squat." *International Shipbuilding Progress*, 26(294), 44–47.
- Barrass, C. and Derrett, D. (2012). *Ship Stability for Masters and Mates*. Butterworth-Heinemann.
- Bi, Q. and Toorman, E. (2015). "Mixed-sediment transport modelling in scheldt estuary with a physics-based bottom friction law." *Ocean Dynamics*, 65(4), 555–587.
- Bonneton, P., Bonneton, N., Parisot, J.-P., and Castelle, B. (2015). "Tidal bore dynamics in funnel-shaped estuaries." *Journal of Geophysical Research: Oceans*, 120(2), 923–941.
- Briggs, M., Vantorre, M., Uliczka, K., and Debaillon, P. (2009). *Prediction of squat for underkeel clearance*. World Scientific.
- Brown, J. and Davies, A. (2010). "Flood/ebb tidal asymmetry in a shallow sandy estuary and the impact on net sand transport." *Geomorphology*, 114(3), 431–439.
- Debaillon, P. (2010). "Numerical investigation to predict ship squat." *Journal of Ship Research*, 54(2), 133–140.
- Delefortrie, G., Vantorre, M., and Eloit, K. (2005). "Modelling navigation in muddy areas through captive model tests." *Journal of Marine Science and Technology*, 10, 188–202.
- Delefortrie, G., Vantorre, M., Eloit, K., Verwilligen, J., and Lataire, E. (2010). "Squat prediction in muddy navigation areas." *Ocean Engineering*, 37(16), 1464–1476.
- Doxaran, D., Froidefond, J.-M., Castaing, P., and Babin, M. (2009). "Dynamics of the turbidity maximum zone in a macrotidal estuary (the gironde, france): Observations from field and modis satellite data." *Estuarine, Coastal and Shelf Science*, 81(3), 321–332.

501 Eloot, K., Vantorre, M., Richter, J., and Verwilligen, J. (2009). "Development of decision  
502 supporting tools for determining tidal windows for deep-drafted vessels." *Marine navi-  
503 gation and safety of sea transportation*, A. Weintrit, ed., CRC Press, 227–234.

504 Eryuzlu, N. E., Cao, Y. L., and D’Agnolo, F. (1994). "Underkeel requirements for large  
505 vessels in shallow waterways." *Proc. 28th Int. Navi. Cong., PIANC*, Sevilla, Spain, 17–  
506 25.

507 Fagerholt, K. and Lindstad, H. (2007). "Turborouter: An interactive optimisation-based  
508 decision support system for ship routing and scheduling." *Maritime Economics and Lo-  
509 gistics*, 9(3), 214–233.

510 Hervouet, J.-M. (2007). *Hydrodynamics of Free Surface Flows: Modelling with the finite  
511 element method*. John Wiley & Sons, Ltd.

512 Huuska, O. (1976). "On the evaluation of underkeel clearances in finnish waterways.

513 Jalón-Rojas, I., Schmidt, S., and Sottolichio, A. (2015). "Turbidity in the fluvial gironde  
514 estuary (southwest france) based on 10-year continuous monitoring: Sensitivity to hy-  
515 drological conditions." *Hydrology and Earth System Sciences*, 19(6), 2805–2819.

516 Jalón-Rojas, I., Sottolichio, A., Hanquiez, V., Fort, A., and Schmidt, S. (2018). "To what  
517 extent multidecadal changes in morphology and fluvial discharge impact tide in a con-  
518 vergent (turbid) tidal river." *Journal of Geophysical Research: Oceans*, 123(5), 3241–  
519 3258.

520 Kaidi, S., Lefrançois, E., and Smaoui, H. (2020). "Numerical modelling of the muddy layer  
521 effect on ship’s resistance and squat." *Ocean Engineering*, 199.

522 Kim, S.-H. and Lee, K.-K. (1997). "An optimization-based decision support system for ship  
523 scheduling." *Computers and Industrial Engineering*, 33(3-4), 689–692.

524 Lam, J. S. L. and Dai, J. (2012). "A decision support system for port selection." *Trans-  
525 portation Planning and Technology*, 35(4), 509–524.

526 Lataire, E. and Vantorre, M. (2017). "Hydrodynamic interaction between ships and re-  
527 stricted waterways." *Transactions of the Royal Institution of Naval Architects Part A:*

528 *International Journal of Maritime Engineering*, 159, 77–87.

529 Lazarowska, A. (2016). “A new deterministic approach in a decision support system for  
530 ship’s trajectory planning.” *Expert Systems with Applications*, 71.

531 Mar-Ortiz, J., Gracia, M., and Castillo-García, N. (2018). *Challenges in the Design of*  
532 *Decision Support Systems for Port and Maritime Supply Chains*. Springer, 49–71.

533 Pairaud, I., Lyard, F., Auclair, F., Letellier, T., and Marsaleix, P. (2008). “Dynamics of the  
534 semi-diurnal and quarter-diurnal internal tides in the bay of Biscay. part 1: Barotropic  
535 tides.” *Continental Shelf Research*, 28(10-11), 1294–1315.

536 Parker, B. and Huff, L. (1998). “Modern under-keel clearance management.” *International*  
537 *Hydrographic Review*, 75(2), 143–166.

538 Römisch, K. (1989). “Empfehlungen zur Bemessung von Hafeneinfahrten.” *Wasser-*  
539 *bauliche Mitteilungen der Technischen Universität Dresden*, 1, 39–63.

540 Ross, L. and Sottolichio, A. (2016). “Subtidal variability of sea level in a macrotidal and  
541 convergent estuary.” *Continental Shelf Research*, 131, 28–41.

542 Santoro, P., Fossati, M., and Piedra-Cueva, I. (2013). “Study of the meteorological tide in  
543 the Río de la Plata.” *Continental Shelf Research*, 60, 51–63.

544 Schmidt, S. (2016). *Le réseau MAGEST : bilan de 10 ans de suivi haute-fréquence de la*  
545 *qualité des eaux de l’estuaire de la Gironde*. CNRS Éditions.

546 Sottolichio, A. and Castaing, P. (1999). “A synthesis on seasonal dynamics of highly-  
547 concentrated structures in the Gironde estuary.” *Comptes Rendus de l’Académie de*  
548 *Sciences - Serie IIa: Sciences de la Terre et des Planètes*, 329(11), 795–800.

549 Sys, C., Blauwens, G., Omeij, E., Van De Voorde, E., and Witlox, F. (2008). “In search  
550 of the link between ship size and operations.” *Transportation Planning and Technology*,  
551 31(4), 435–463.

552 Tournadre, J. (2014). “Anthropogenic pressure on the open ocean: The growth of ship traf-  
553 fic revealed by altimeter data analysis.” *Geophysical Research Letters*, 41(22), 7924–  
554 7932 cited by 54.

555 Van, L. A. (2012). "Numerical modelling of sand-mud mixtures settling and transport pro-  
556 cesses: application to morphodynamic of the gironde estuary (france)." Ph.D. thesis,  
557 Université Paris-Est, Université Paris-Est.

558 van Maanen, B. and Sottolichio, A. (2018). "Hydro- and sediment dynamics in the gironde  
559 estuary (france): Sensitivity to seasonal variations in river inflow and sea level rise."  
560 *Continental Shelf Research*, 165, 37–50.

561 Vantorre, M., Candries, M., and Verwilligen, J. (2013). "Optimization of tidal windows for  
562 deep-drafted vessels by means of protoel." *Next Generation Nautical Traffic Models*,  
563 *International workshop, Papers*, 10.

564 Vantorre, M., Eloit, K., Delefortrie, G., Lataire, E., Candries, M., and Verwilligen, J.  
565 (2017). *Maneuvering in Shallow and Confined Water*. John Wiley & Sons.

566 Yoshimura, Y. (1986). "Mathematical model for the maneuvering ship motion in shallow  
567 water." *J. Kansai Soc. Nav. Arch. Japan*, 1(200).

568 Zou, L. and Larsson, L. (2013). "Computational fluid dynamics (cfd) prediction of bank  
569 effects including verification and validation." *Journal of Marine Science and Technology*  
570 *(Japan)*, 18(3), 310–323.

571

**List of Tables**

572

1 Model performance parameters (Root Mean Square Error and Skill Score)

573

for water levels with astronomical tide (AT) and NavTEL predictions at all

574

tidal gages. . . . . 27

**TABLE 1.** Model performance parameters (Root Mean Square Error and Skill Score) for water levels with astronomical tide (AT) and NavTEL predictions at all tidal gages.

Tidal gages	RMSE		SS	
	AT	NavTEL	AT	NavTEL
Le Verdon (8)	0.13	0.15	0.987	0.983
Richard (7)	0.15	0.17	0.939	0.982
Lamena (6)	0.18	0.18	0.983	0.981
Pauillac (5)	0.19	0.20	0.981	0.980
Le Marquis (2)	0.23	0.15	0.977	0.990
Bordeaux (0)	0.31	0.22	0.964	0.982



575 **List of Figures**

576 1 (a) Location map of the study area in the southwest of France and (b) the  
577 Gironde Estuary and its tributaries the Garonne and the Dordogne Rivers.  
578 The navigation channel is characterized by a dash grey line and stretches  
579 from the estuary mouth to the port of Bordeaux in the Garonne River, the  
580 main tributary. Black stars show tidal gauges located along the Estuary and  
581 blue squares show harbors including the Bordeaux Harbor. Depth-limited  
582 locations are represented by orange circles. (c) Numerical domain extend-  
583 ing from the maritime part to the Dordogne River and the Garonne River.  
584 (d) The mesh is unstructured and composed of triangular elements with el-  
585 element sizes ranging from 80 m to 300 m for refined areas and the maritime  
586 part, respectively. (e) The Turbidity Maximum Zone (TMZ) is reproduced  
587 with a mud deposit of  $2.6 \times 10^6$  tons in the central estuary and depicted by  
588 orange areas. . . . . 30

589 2 Flow chart of NavTEL, a decision support tool used to schedule ship route  
590 and manage underkeel clearance in estuarine channels. NavTEL has a  
591 modular structure and a kernel composed of NAVIRE and TELBOT mod-  
592 ules. The TELBOT module prepares and runs daily simulations with the  
593 TELEMAC-MASCARET modeling system. Numerical simulations incorpo-  
594 rate real-time variations of river discharge and storm surges. The NAVIRE  
595 module post-processes the numerical outputs to provide the safest route  
596 and to predict allowable drafts. In the Figure, the kernel and the optional  
597 modules of NavTEL are indicated by gray and green boxes. NavTEL is  
598 written in Python 2.7 and is available as an open-source code at [https:](https://gitlab.com/orseausy/navtel)  
599 [//gitlab.com/orseausy/navtel](https://gitlab.com/orseausy/navtel). . . . . 31

600	3	Comparison between measured and predicted free surface (m) with astronomical tide (AT) (a-c) and with NavTEL simulations (d-f) at Le Verdon, Pauillac and Bordeaux stations. . . . .	32
601			
602			
603	4	Comparison of the difference in time of high water between measurements and predictions at (a) Le Verdon, (b) Pauillac and (c) Bordeaux stations. Predictions with only astronomical tide (AT) and with NavTEL are represented with black plus signs and red circles, respectively. . . . .	33
604			
605			
606			
607	5	Temporal mean of the salinity over the numerical domain for the predicted period of the 03/19/2020. At this period, the salt intrusion is restricted to the lower estuary at downstream Richard station. See Fig. 1b for locations. . . . .	34
608			
609			
610	6	Variations of the allowable draft along the navigation channel and for the predicted period from the 03/19/2020. The figure was generated for an arrival at the Bassens Aval terminal and for a ship draft of 10 m. The black line indicates the start time for the safest route as well as the critical location where the maximum allowable draft where found. . . . .	35
611			
612			
613			
614			
615	7	Variations of the velocity (a), the salinity (b), the suspended particulate matter (c) and the predicted squat (d) along the navigation channel and for the safest route. The figure was generated for an arrival at the Bassens Aval terminal and for a ship draft of 8.3 m. . . . .	36
616			
617			
618			

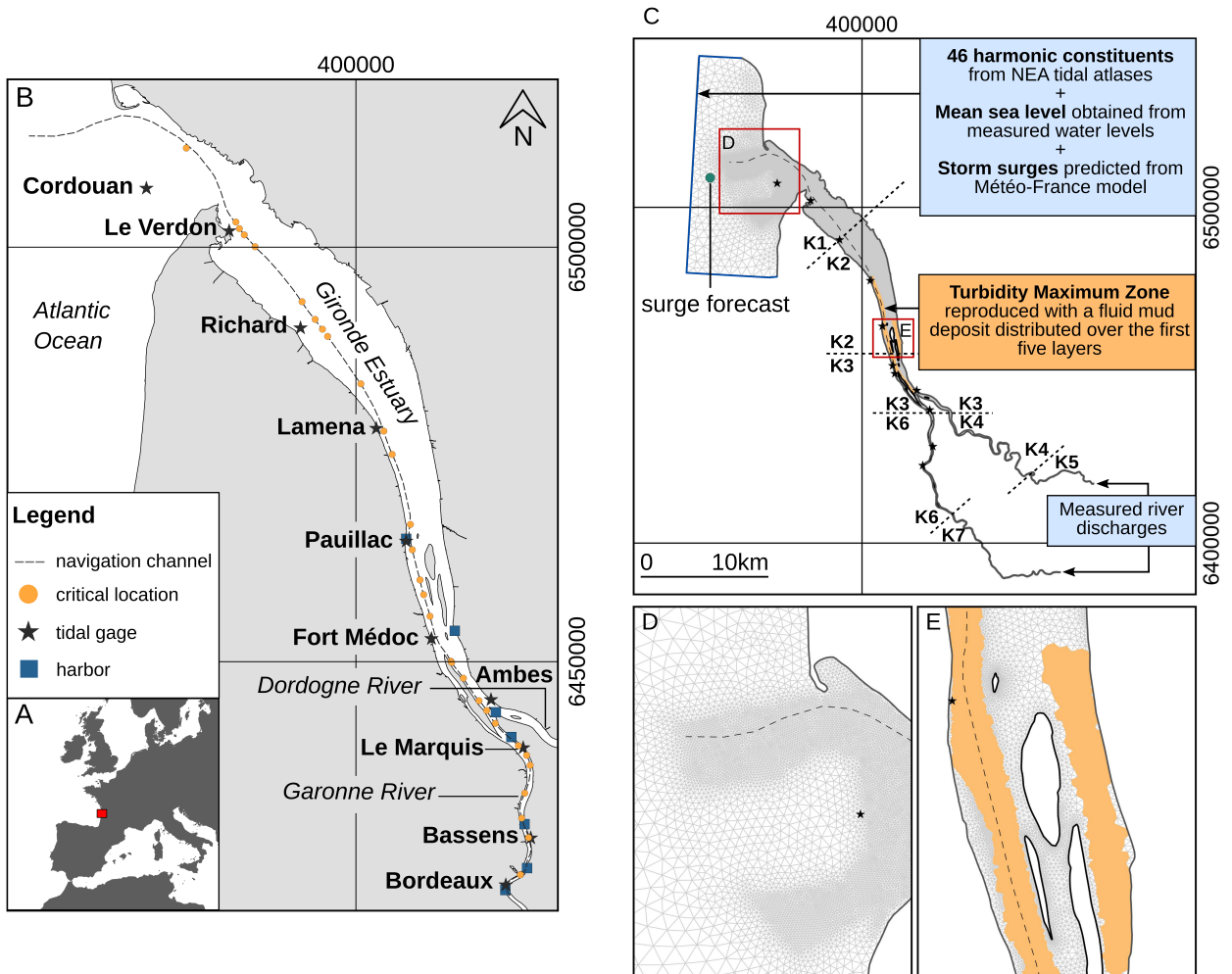


**Fig. 1.** (a) Location map of the study area in the southwest of France and (b) the Gironde Estuary and its tributaries the Garonne and the Dordogne Rivers. The navigation channel is characterized by a dash grey line and stretches from the estuary mouth to the port of Bordeaux in the Garonne River, the main tributary. Black stars show tidal gauges located along the Estuary and blue squares show harbors including the Bordeaux Harbor. Depth-limited locations are represented by orange circles. (c) Numerical domain extending from the maritime part to the Dordogne River and the Garonne River. (d) The mesh is unstructured and composed of triangular elements with element sizes ranging from 80 m to 300 m for refined areas and the maritime part, respectively. (e) The Turbidity Maximum Zone (TMZ) is reproduced with a mud deposit of  $2.6 \times 10^6$  tons in the central estuary and depicted by orange areas.

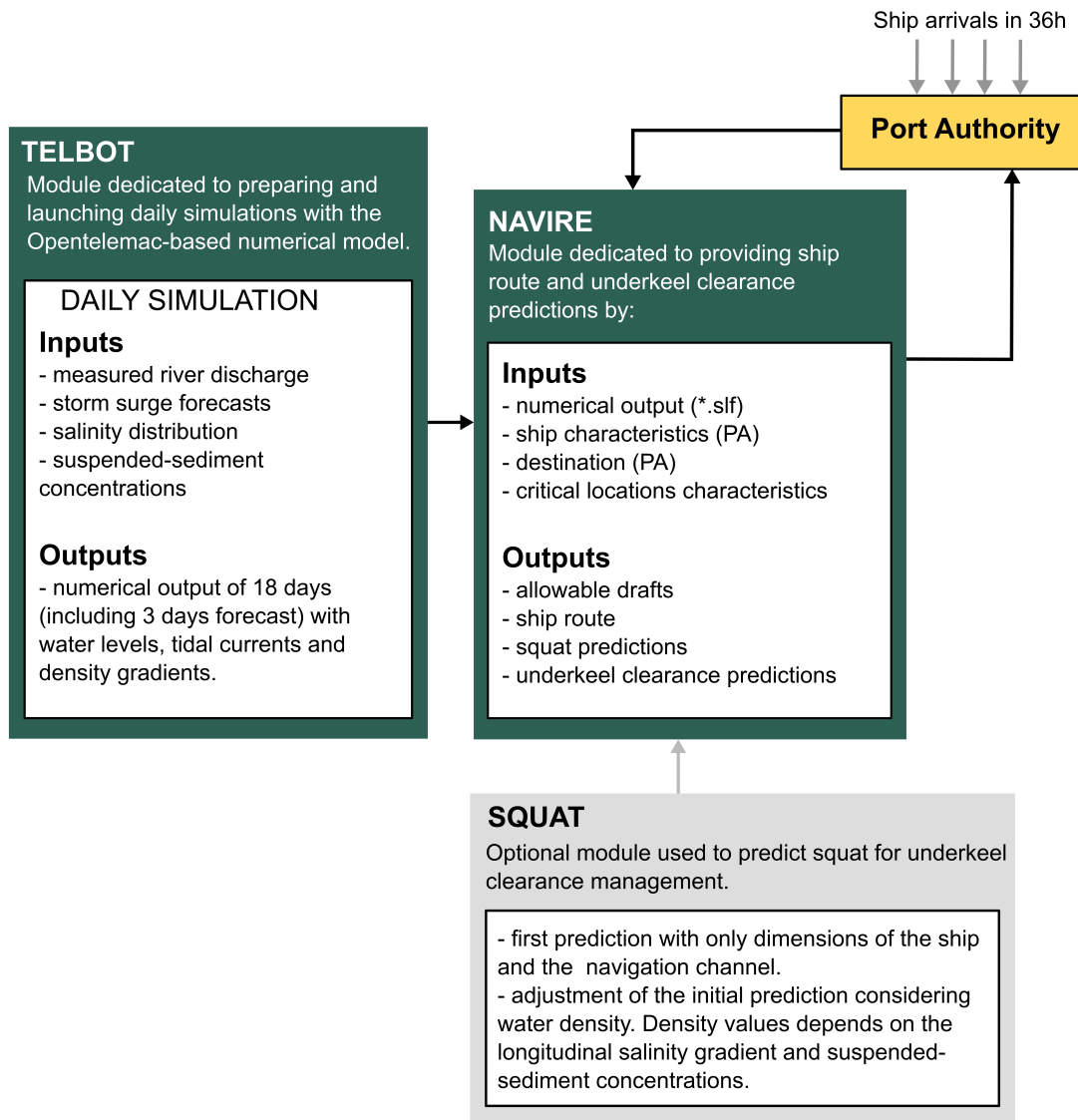


**Fig. 2.** Flow chart of NavTEL, a decision support tool used to schedule ship route and manage underkeel clearance in estuarine channels. NavTEL has a modular structure and a kernel composed of NAVIRE and TELBOT modules. The TELBOT module prepares and runs daily simulations with the TELEMAC-MASCARET modeling system. Numerical simulations incorporate real-time variations of river discharge and storm surges. The NAVIRE module post-processes the numerical outputs to provide the safest route and to predict allowable drafts. In the Figure, the kernel and the optional modules of NavTEL are indicated by gray and green boxes. NavTEL is written in Python 2.7 and is available as an open-source code at <https://gitlab.com/orseausy/navtel>.

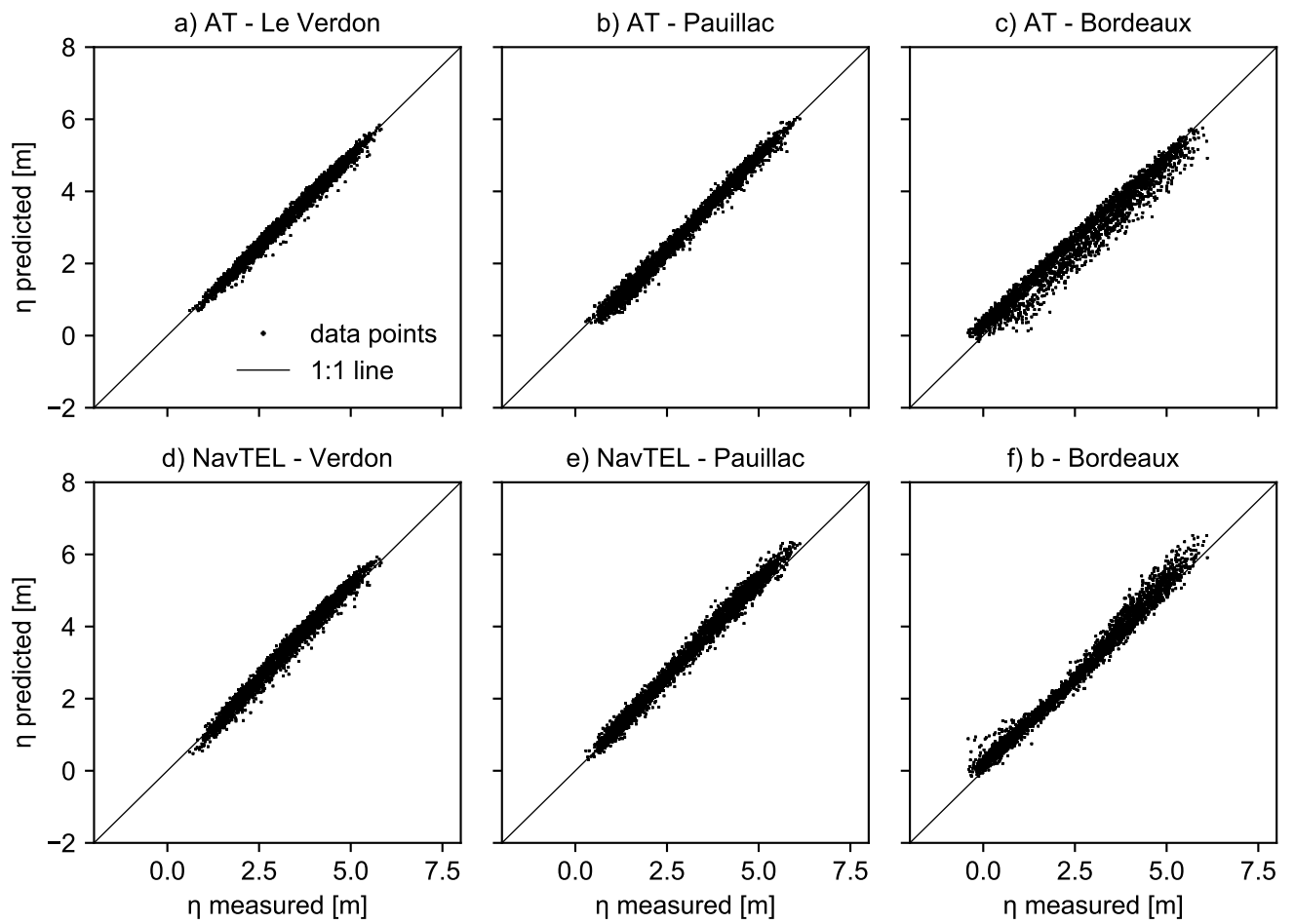


**Fig. 3.** Comparison between measured and predicted free surface (m) with astronomical tide (AT) (a-c) and with NavTEL simulations (d-f) at Le Verdon, Pauillac and Bordeaux stations.

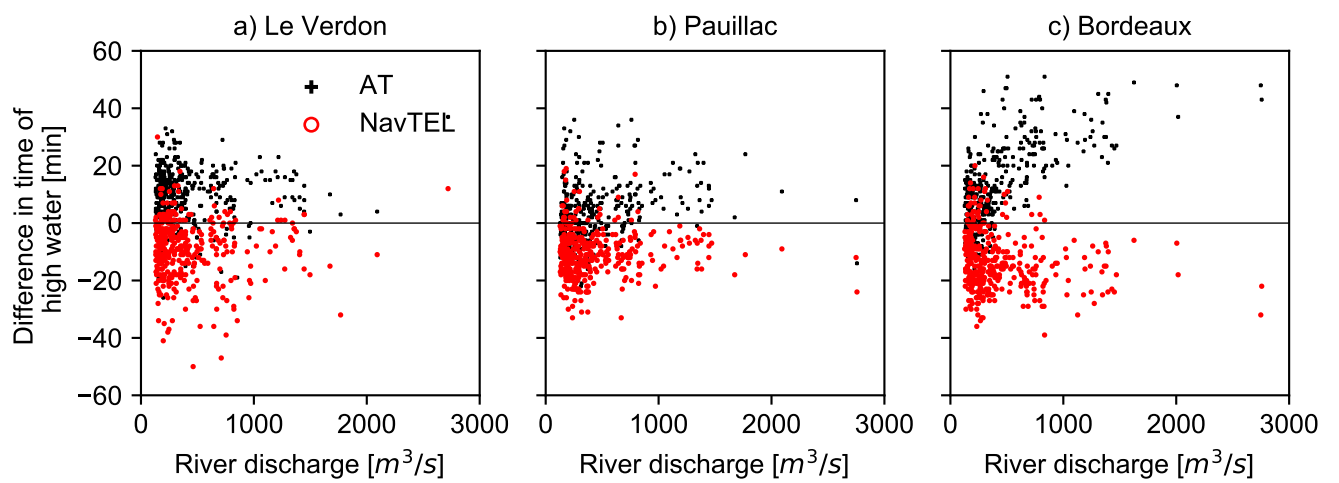


**Fig. 4.** Comparison of the difference in time of high water between measurements and predictions at (a) Le Verdon, (b) Pauillac and (c) Bordeaux stations. Predictions with only astronomical tide (AT) and with NavTEL are represented with black plus signs and red circles, respectively.

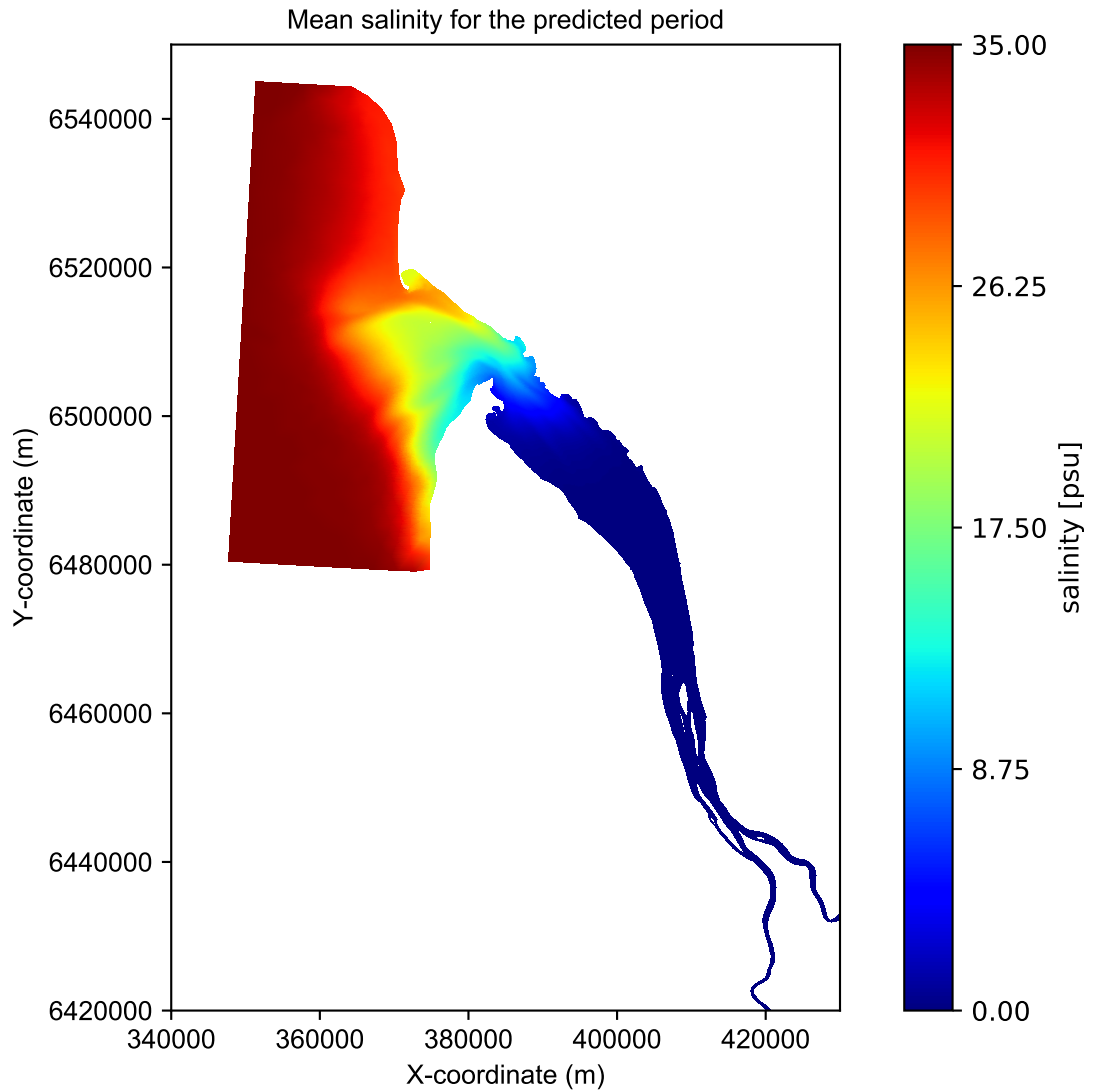


**Fig. 5.** Temporal mean of the salinity over the numerical domain for the predicted period of the 03/19/2020. At this period, the salt intrusion is restricted to the lower estuary at downstream Richard station. See Fig. 1b for locations.

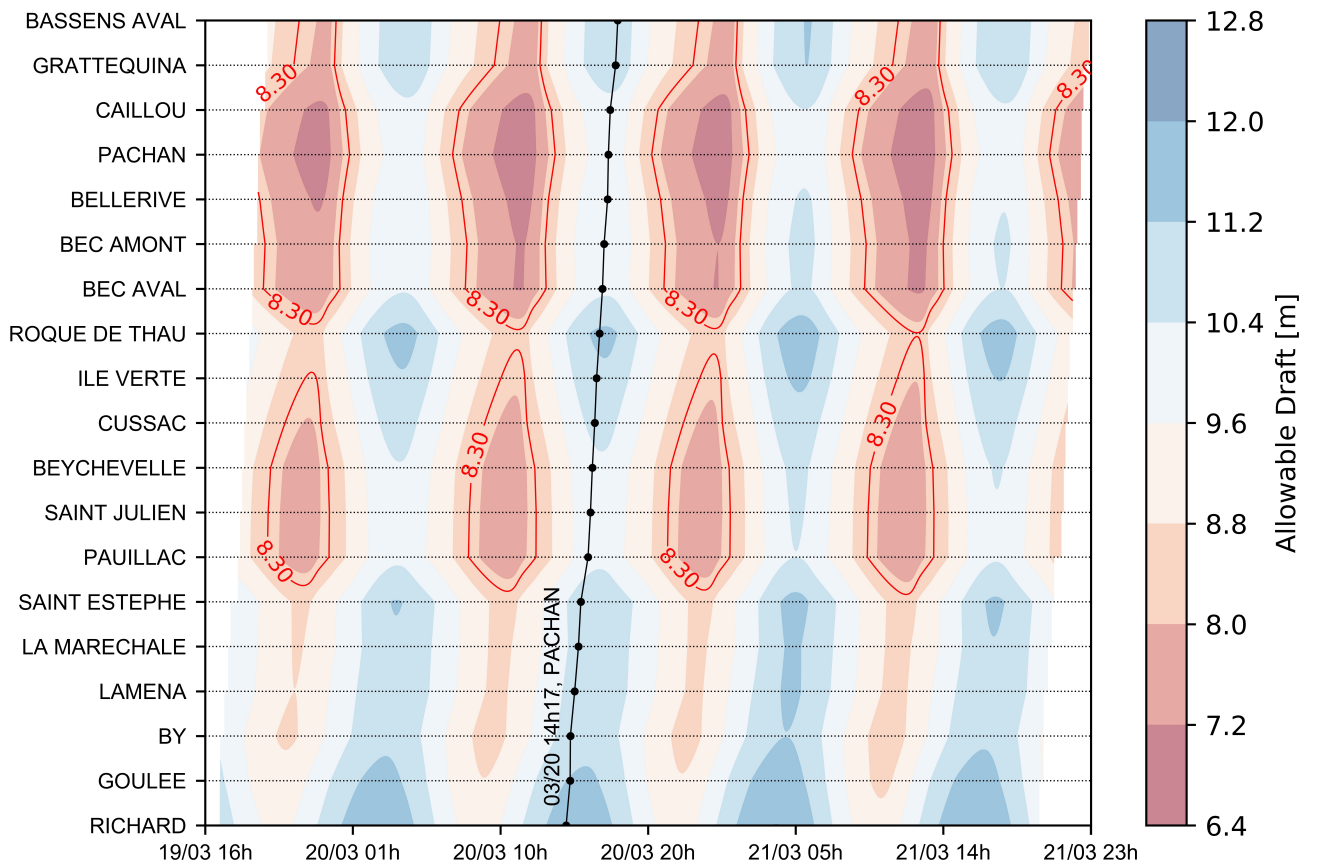


**Fig. 6.** Variations of the allowable draft along the navigation channel and for the predicted period from the 03/19/2020. The figure was generated for an arrival at the Bassens Aval terminal and for a ship draft of 10 m. The black line indicates the start time for the safest route as well as the critical location where the maximum allowable draft where found.



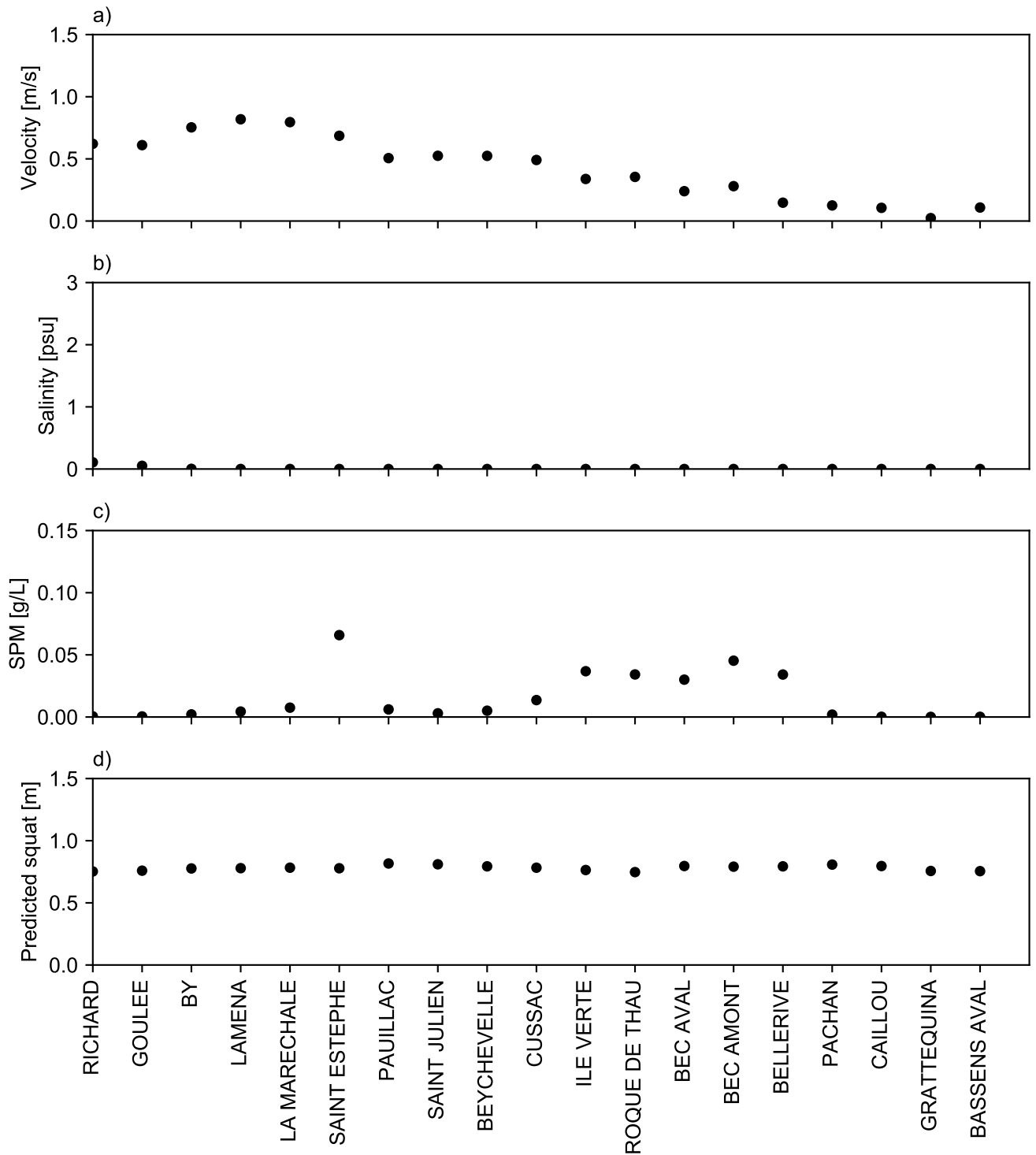


**Fig. 7.** Variations of the velocity (a), the salinity (b), the suspended particulate matter (c) and the predicted squat (d) along the navigation channel and for the safest route. The figure was generated for an arrival at the Bassens Aval terminal and for a ship draft of 8.3 m.